Both maltose-binding protein and ATP are required for nucleotide-binding domain closure in the intact maltose ABC transporter

Cedric Orelle*, Tulin Ayvaz†, R. Michael Everly*, Candice S. Klug‡, and Amy L. Davidson*§

*Department of Chemistry, Purdue University, 560 Oval Drive, West Lafayette, IN 47907; †Molecular Virology and Microbiology, Baylor College of Medicine, 1 Baylor Plaza, Houston, TX 77030; and ‡Department of Biophysics, Medical College of Wisconsin, 8701 Watertown Plank Road, Milwaukee, WI 53226

Edited by Douglas C. Rees, California Institute of Technology, Pasadena, CA, and approved June 6, 2008 (received for review April 20, 2008)

The maltose transporter $MalFGK_2$ of *Escherichia coli* is a member of the ATP-binding cassette superfamily. A periplasmic maltose-binding protein (MBP) delivers maltose to $MalFGK_2$ and stimulates its ATPase activity. Site-directed spin labeling EPR spectroscopy was used to study the opening and closing of the nucleotide-binding interface of $MalFGK_2$ during the catalytic cycle. In the intact transporter, closure of the interface coincides not just with the binding of ATP, as seen with isolated nucleotide-binding domains, but requires both MBP and ATP, implying that MBP stimulates ATPase activity by promoting the closure of the nucleotide-binding interface. After ATP hydrolysis, with MgADP and MBP bound, the nucleotide-binding interface resides in a semi-open configuration distinct from the fully open configuration seen in the absence of any ligand. We propose that P_i release coincides with the reorientation of transmembrane helices to an inward-facing conformation and the final step of maltose translocation into the cell.

catalytic cycle | conformational change | EPR | membrane protein | P-glycoprotein

ATP-binding cassette (ABC) proteins make up one of the largest superfamilies of proteins and are found in all living organisms. Most are membrane transporters that couple ATP hydrolysis to import or export of a large variety of substrates (1). Some transporters display high specificity for substrates, including those that transport sugars and amino acids, whereas others are less specific. Overexpression of efflux pumps displaying broad substrate specificity is a cause of multidrug resistance in cancer cells (2) and microorganisms (3). Genetic defects in ABC transporters are also associated with severe human diseases including cystic fibrosis and adrenoleukodystrophy (4). Hence, understanding their mechanism of action is a major medical challenge. ABC transporters minimally contain two transmembrane spanning domains that provide a substrate-specific pathway across the membrane and two nucleotide-binding domains (NBDs) that energize the transporter (5). The last decade offered major advances in the understanding of their structure and mechanism of action. Many isolated NBDs behave as monomers in solution and dimerize on ATP binding (6), adopting a head-to-tail configuration with two ATP molecules sandwiched between the nucleotide-binding Walker A motif of one NBD and the family signature or LSGGQ motif of the second NBD (7, 8). This observation led to the idea that both ATP-driven dimerization of NBDs and ATP hydrolysis could participate in the substrate transport cycle. Structural and biochemical analysis of intact ABC importers indicate that NBDs "*in situ*" experience a similar ATP-dependent closure of the nucleotide-binding interface (Fig. 1*A*) although they maintain some contact with each other even in the absence of nucleotide (9, 10). Vanadate-photocleavage experiments, performed in the intact maltose transporter, suggest that ATP hydrolysis occurs in the closed conformation when residues in both the Walker A and LSGGQ motifs closely contact the γ-phosphate of ATP (11). In addition, mutations in the signature motif strongly inhibit the ATPase activity of ABC proteins (12–14).

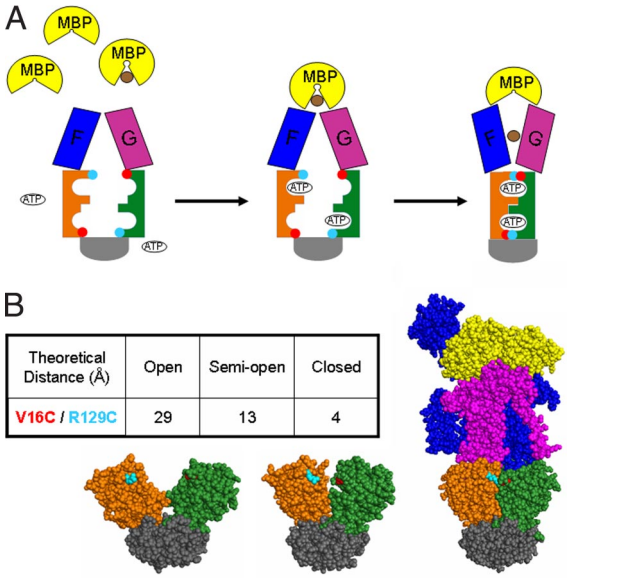

Fig. 1. Nucleotide-binding interface closure during the catalytic cycle. (*A*) General scheme of conformational changes in the maltose transporter. Maltose is represented in brown and MBP in yellow. Transmembrane subunits MalF and MalG are shown in blue and purple, respectively. MalK NBDs are orange and green, and both of their regulatory domains are gray. Red and cyan circles represent the cysteine mutations that were introduced in MalK (V16C and R129C). (*B*) Location of V16C (red) and R129C (cyan) mutations in different conformational states of the MalK dimer. (*Left*) Open MalK dimer (1Q1E). (*Center*) Semi-open MalK dimer (1Q1B). (*Right*) Closed, ATP-bound MalK dimer in complex with MalF, MalG, and MBP (2R6G) (10, 18). The table inset indicates the distances (Å) between the side chains of V16 and R129 in the crystals.

We used site-directed spin labeling (SDSL) EPR spectroscopy to study the dynamics of the nucleotide-binding interface during the catalytic cycle of the intact *Escherichia coli* maltose transporter. This ABC transporter, $MalFGK_2$, is a complex of two membrane-spanning subunits named MalF and MalG and two NBDs named MalK. A periplasmic maltose-binding protein (MBP) acts as a maltose receptor and interacts with the transporter complex to deliver the substrate (15). MBP also stimulates

Author contributions: C.O. and A.L.D. designed research; C.O. and T.A. performed research; R.M.E. contributed new reagents/analytic tools; C.O., C.S.K., and A.L.D. analyzed data; and C.O., C.S.K., and A.L.D. wrote the paper.

The authors declare no conflict of interest.

This article is a PNAS Direct Submission.

§To whom correspondence should be addressed. E-mail: adavidso@purdue.edu.

Table 1. ATPase activities of spin-labeled transporters measured in the presence or absence of MBP

Transporter	ATPase activity, nmol·min^{-1}·mg^{-1}	
	−MBP	+MBP
Cys-less	0	2,100
V16C	38	1,800
R129C	12	1,330
V16C/R129C	0	1,150
W13C	0	1,100

Representative determinations on a single preparation are reported and similar results were obtained in subsequent preparations (with <10% variability).

the ATPase activity of $MalFGK_2$, ensuring that maltose transport is coupled to ATP hydrolysis (16, 17). The mechanism by which MBP stimulates ATPase activity is not fully understood, and two different scenarios may occur. First, ATP binding may trigger closure even in the absence of MBP, but binding of MBP, opening of MBP, and/or release of maltose into the transporter may be required to properly orient catalytic residues in the ATP-binding sites. This model is consistent with the fact that ATP binding triggers closure in isolated NBDs (6, 7, 18–20) and may explain why the ATPase activity of isolated NBDs is often low compared with intact transporters (21). Second, in the absence of MBP, the binding of ATP may fail to trigger closure of the nucleotide-binding interface, thereby preventing ATP hydrolysis. Our results support the latter scenario in which binding of both MBP and ATP initiate a concerted conformational change that opens MBP as MalK closes to hydrolyze ATP. We also found an intermediate state in the catalytic cycle that brings insight into the mechanism of maltose transport.

Results

Introducing V16C/R129C in MalK for SDSL and EPR Spectroscopy. A cysteine-free $MalFGK_2$ with improved levels of expression was created (see *Materials and Methods*). To detect the closure and opening of the nucleotide-binding interface in the intact transporter, two cysteines were introduced into MalK at sites that, according to the structures (10, 18), are close to each other across the closed dimer interface and distant within a MalK monomer (red and cyan circles in Fig. 1*A*). Based on several parameters including distance, labeling efficiency, and functionality, we selected the V16C/R129C pair for study (Fig. 1*B*). Each single mutant labeled with 1-oxyl-2,2,5,5-tetramethyl-3-pyrroline-3-methyl methanethiosulfonate spin label (MTSL) at 95% efficiency, and the double mutant V16C/R129C labeled with 85–90% efficiency. High labeling efficiency is important to calculate accurate distances. Both single and double cysteine mutants were able to complement a deletion of the *malK* in *E. coli*. The ATPase activities of the purified and reconstituted spin-labeled mutant transporters are reported in Table 1. Notably, the spin-labeled V16C/R129C double mutant retained 55–60% of the ATPase activity of the cysteine-free transporter and excellent stimulation by MBP.

The distances between the native side chains of residues V16 and R129, in opposing subunits at their closest point of contact, are 4 Å in the structure of the closed MalK dimer (10), 13 Å in the symmetrical semi-open structure of MalK (18), and 29 Å in the fully open structure of MalK (18) (Fig. 1*B*). Continuous wave EPR spectroscopy can accurately measure distances between 8 and 25 Å (22). Importantly, the V16 and R129 side chains within the MalK monomer remain >39 Å apart in all conformations, and the distances between identical residues in opposing subunits are >35 Å in all conformations, ensuring that any distance changes detected by EPR will be across the dimer interface, thus reflecting the opening and closing of the nucleotide-binding interface.

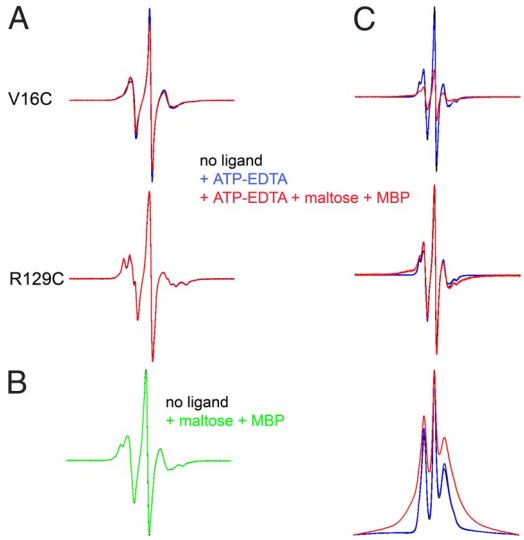

Fig. 2. Effect of ATP and MBP on EPR spectra of single mutants V16C and R129C (*A*) and V16C/R129C double mutant (*B* and *C*). (*A*) 150 G wide EPR spectra of V16C and R129C. Spectra are colored as indicated in the figure. (*B*) 150 G wide spectra of V16C/R129C transporter alone (black) or in the presence of maltose-MBP (green). (*C*) 250 G wide spectra of V16C/R129C transporter with the same color designations as in *A*. (*Top*) Graphic represents data normalized to the same number of spins (double integration of signal). (*Middle*) Same data normalized to maximal amplitude. (*Bottom*) First integral of spectra normalized to maximum amplitude. Note that broadening should result solely from spin–spin interaction because experiments on single mutants (*A*) indicate that ligand addition does not significantly modify the mobility of the spin labels at these positions.

Visualizing Closure of the MalK Dimer: Both ATP and MBP Are Required to Close the MalK Dimer in the Intact Transporter. We studied the effect of maltose transporter ligands (ATP or ATP+maltose+MBP) on the EPR spectra of spin-labeled V16C and R129C single mutants. EDTA was added to ATP to chelate the Mg^{2+} and to prevent ATP hydrolysis. We observed no changes in the shape of the R129C spectrum and only slight changes in the V16C spectrum on addition of ATP or ATP+maltose+MBP (Fig. 2*A*). Therefore, these ligands do not significantly change the mobility of the probes at these positions, making this system ideal to study changes in spin–spin interaction in the V16C/R129C double mutant.

The spectrum of a doubly labeled protein is a composite of the spectra of the noninteracting single mutants, onto which is superimposed the spectrum that results from the interaction of the spins. The spin–spin interaction depends on the distance between the spin labels and results in a dipolar broadening of the spectrum. The magnetic dipolar interactions between two spin labels within 25 Å can be analyzed in terms of interspin distance by using a spectral deconvolution program (23), which can distinguish between multiple discrete distances, a single distance distribution, or a continuum of distances. Comparative analysis of the EPR spectrum for the doubly labeled V16C/R129C mutant and the spectral sum of each single mutant did not reveal any spin–spin interaction (data not shown), showing that the nitroxide probes are unambiguously >20 Å apart with no ligands present. Thus, in the resting state of the intact transporter, MalK appears to adopt an open conformation similar to that seen in the ligand-free crystal structures of isolated MalK (18) (see also Fig. 1*B Bottom Left* and *Bottom Center*). The addition of MBP and maltose had no effect on the spectrum (Fig. 2*B*), indicating

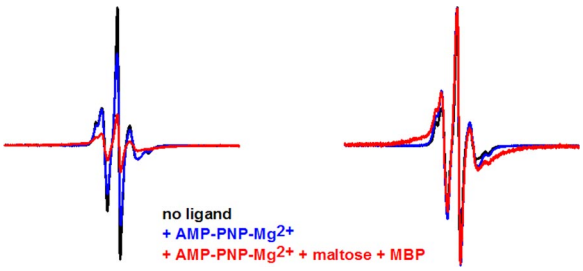

Fig. 3. Effect of AMP-PNP-Mg^{2+} and MBP on V16C/R129C transporter. Spectra (250 G) are colored as indicated in the figure. Experimental spectra are normalized to the same number of spins (*Left*) and maximum amplitude (*Right*).

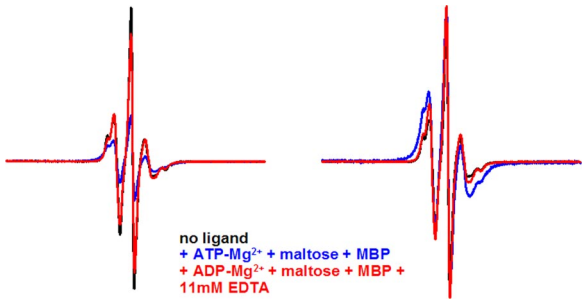

Fig. 4. Reopening of the nucleotide-binding interface in V16C/R129C transporter. Spectra (250 G) are colored as indicated. Experimental spectra are normalized to the same number of spins (*Left*) and maximum amplitude (*Right*).

that MBP by itself cannot close the nucleotide-binding interface of $MalFGK_2$. Next, we investigated whether ATP alone could promote closure in the intact transporter. As shown in Fig. 2*C*, ATP alone is unable to induce any significant closure of the nucleotide-binding interface (compare black and blue lines). However, the addition of ATP and maltose+MBP (red line) triggered significant spin–spin interaction as visualized by the decrease in amplitude of the center peak and the broadening of the spectral lineshape (see also the broadening of the absorption spectrum on the bottom of Fig. 2*C*). Analysis of the spectrum indicates a distance of 7–8 Å between spin labels for ≈60% of the total population with the reminder still >20Å. Because under labeling (85–90% labeling efficiency for the double mutant) contributes a population of noninteracting spins, we estimate that 70–75% of the doubly labeled population has closed. Taken together, these data demonstrated that both ATP and MBP are required for closure of the nucleotide-binding interface in the intact maltose ABC transporter. MBP in the absence of maltose is also able to induce closure of the nucleotide-binding interface in the presence of ATP (data not shown) just as maltose-free MBP stimulates low rates of ATP hydrolysis (16).

Binding of AMP-PNP-Mg^{2+} Does Not Close the Nucleotide-Binding Interface in the Absence of Maltose-MBP. AMP-PNP is a nonhydrolyzable analogue of ATP, and we used this analogue in the presence of the Mg^{2+} cofactor to examine the effect on NBD closure. Importantly, EPR studies have shown that binding of either ATP or AMP-PNP-Mg^{2+} to $MalFGK_2$ triggers the opening of MBP in the intact transporter (15). Like ATP, AMP-PNP-Mg^{2+} could not close the nucleotide-binding interface (Fig. 3) but did generate a small population of distances at 17–18 Å, not seen in the ligand-free or ATP-bound transporters. Subsequent addition of maltose-MBP again promoted strong spin–spin interaction with a distance centered at 7–8 Å for ≈80% of the total population, demonstrating that MBP is required for closure even with Mg^{2+} present. Given that labeling was incomplete, it is likely that at least 90% of the doubly labeled population is fully closed.

Opening of the MalK Dimer During the Catalytic Cycle of the Intact Maltose Transporter. According to a well accepted model (6), ATP binding promotes closure of the nucleotide-binding interface, and ATP hydrolysis promotes its reopening. We tested whether the addition of Mg^{2+} to allow hydrolysis by transporters that were closed in the presence of ATP and maltose-MBP would reopen the nucleotide-binding interface. Strikingly, the addition of Mg^{2+} generated a conformation that appeared intermediate between the open resting state and the closed ATP-bound state. The main distance distribution between the spin labels shifted from 7–8 Å to 10–14 Å for ≈60% of the total population, with the remainder displaying no spin–spin interaction (blue spectrum, Fig. 4). Incubation of the transporter with maltose-MBP and ADP-Mg^{2+} generated similar results with 60% of the population at 9–14 Å and another 20% of the population at 16–17 Å (data not shown). These data suggest that, after hydrolysis of ATP in the sample and release of P_i, the transporter preferentially adopts a conformation in which both sites are semi-open, and that the distances between the two positions are more flexible than in the closed conformation. Addition of excess EDTA to transporter complexes incubated with maltose-MBP and either ADP-Mg^{2+} (red spectrum, Fig. 4) or ATP-Mg^{2+} (data not shown) returned both to the fully open state. This result indicates that Mg^{2+} is important to stabilize this intermediate configuration, although it is also possible that the removal of Mg^{2+} decreases the affinity for ADP so that it no longer binds to the transporter.

Dynamics of Interface Closure in a Reconstituted System. Results qualitatively similar to those in detergent solution were obtained after reconstitution of spin-labeled V16C/R129C $MalFGK_2$ into proteoliposomes (compare Fig. 5 *A* and *B*), indicating the motions seen in detergent solution are representative of the transporter in the lipid bilayer. There was no evidence of spin–spin interaction in the resting state, indicating that the nucleotide-binding interface is open. Both AMP-PNP-Mg^{2+} and maltose-MBP were required to close the interface. Because the ATPase activity of the transporter in the absence of MBP is much lower in proteoliposomes (Table 1) than in detergent (24), it was also possible to demonstrate the failure of ATP-Mg^{2+} to stabilize the closed conformation of the reconstituted trans-

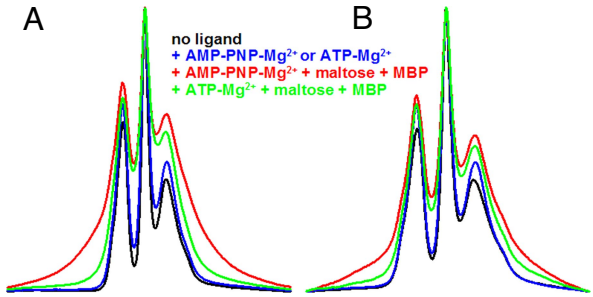

Fig. 5. Effects of ligands on V16C/R129C either in detergent (*A*) or in proteoliposomes (*B*). For clarity, we are showing the first integral representation normalized to maximum amplitude. (*A*) 200 G spectra. AMP-PNP-Mg^{2+} alone was tested (blue). (*B*) 150 G spectra. Both AMP-PNP-Mg^{2+} alone and ATP-Mg^{2+} alone were tested, generating identical spectra (blue). During the course of the experiment, ≈10% of ATP was hydrolyzed, in the absence of MBP. Other colors are as indicated on the figure.

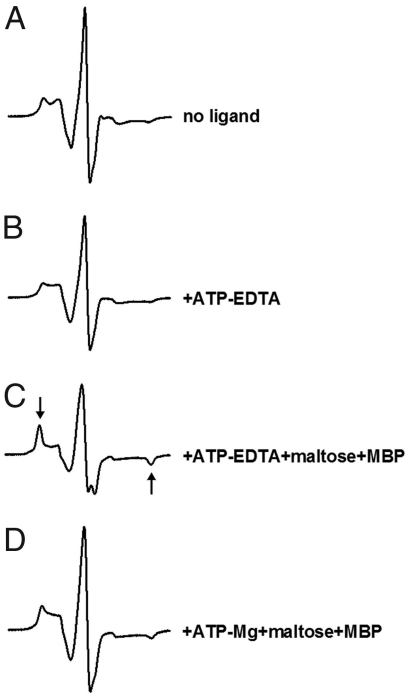

Fig. 6. Effect of ligands on W13C EPR spectra. Spectra are 100 G wide. Arrows indicate the immobilized component.

porter in the absence of MBP (Fig. 5*B*). The spectra obtained in the presence of maltose-MBP and either ATP-Mg^{2+} or ADP-Mg^{2+} reflected partial opening as seen in detergent (Fig. 5*B* or data not shown). Distances measured are not reported because of a higher population of noninteracting spins, most likely because of the limited accessibility of ligands to both sides of the membrane in the vesicles.

Introducing a Single Spin Label into the ATP-Binding Sites of MalK. In ABC proteins, the adenine base of ATP is often stabilized by a stacking interaction with an aromatic amino acid (25). We replaced this residue (W13 in MalK) with a cysteine because we anticipated that nucleotide binding would restrict the motion of the spin label at that position. Surprisingly, the W13C mutant was still functional in transport on MacConkey plates (data not shown). The spin-labeled mutant, reconstituted in proteoliposomes, was also functional (Table 1). The concentration dependence of ATPase activity revealed a K_m for ATP of 0.6 mM in the W13C transporter (with or without spin-labeling) compared with 0.15 mM in the cysteine-free transporter. The addition of 15 mM ATP, in the absence of maltose-MBP, altered the spectrum but not substantially (Fig. 6*B*). In contrast, when maltose-MBP was added to the system, we observed a strong immobilization of spin label (Fig. 6*C*, arrows). These results suggested that MBP promotes a tight positioning of ATP through closure of the nucleotide-binding interface. Finally, the mobility of the W13C EPR spectrum in the posthydrolysis conformation (maltose-MBP + ATP-Mg^{2+}) appeared intermediate between resting state and closed state (Fig. 6*D*) with ≈1/3 of the spin population retaining the immobilized conformation and the remaining population reverting back to a more mobile state.

Discussion

Using SDSL EPR spectroscopy to measure distances across the nucleotide-binding interface, we demonstrated that both ATP (or AMP-PNP-Mg^{2+}) and MBP are required for MalK closure

Table 2. Summary of main EPR distances between positions 16 and 129 in MalK

Ligand	Main distance, Å	MalK conformation
None	>20	Open
Maltose-MBP	>20	Open
ATP	>20	Open
AMP-PNP-Mg^{2+}	>20	Open
ATP + maltose-MBP	7–8	Closed
AMP-PNP-Mg^{2+}+maltose-MBP	7–8	Closed
ATP-Mg^{2+}+maltose-MBP	10–14	Semi-open
ADP-Mg^{2+}+maltose-MBP	9–14	Semi-open

in the intact maltose transporter. These results contrast with those obtained with the isolated MalK dimer (18) where ATP by itself stabilizes the closed form under nonhydrolytic conditions. In the intact transporter, transmembrane subunits impose constraints that prevent MalK closure, and basal ATPase activity is kept low. MBP stimulates the ATPase activity of the transporter by inducing the closure of MalK subunits. A molecular dynamics study on the BtuCD transporter supports the concept that substrate-binding protein is required for NBD closure (26). However, only one nucleotide-binding site closed in their simulation, whereas our data with ATP and AMP-PNP-Mg^{2+} indicate that both nucleotide-binding sites close (75% and 90% of doubly labeled populations were closed, respectively). Although no asymmetry in opening was detected on the addition of Mg^{2+} to promote ATP hydrolysis, the existence of an intermediate with one site open and one site closed, if it exists, may not have been captured because the ATP content of the sample is likely converted into ADP and P_i before a spectrum is recorded.

Although ABC transporters that exhibit higher basal ATPase activity and weaker substrate stimulation may not be as tightly regulated as the maltose transporter, we hypothesize that substrate binding still stimulates ATPase by facilitating the closure of the nucleotide-binding interface in these systems. Albeit rather indirect, the observation that substrates that stimulate the ATPase activity of P-glycoprotein increase the degree to which nucleotides can be trapped in an "occluded conformation" at the dimer interface supports this hypothesis (27).

Enzymes are known to mediate catalysis by stabilizing the transition state, and the closure of the nucleotide-binding interface most likely serves this function. Closure of the interface brings residues from the family signature motif directly into contact with the nucleotide, which may favor the formation of the transition state for ATP hydrolysis. Strong immobilization of the spin label at position 13 suggests that interaction with the signature motif of the opposing subunit could also contribute to catalysis by optimizing the orientation of the ATP molecule with respect to catalytic residues of the nucleotide-binding site.

Our study supports the existence of at least three states of MalK during the catalytic cycle of the intact maltose transporter. In addition to the open and closed conformations already discussed, a distinct posthydrolytic, semi-open intermediate was also seen, either by adding Mg^{2+} to the transporter stabilized in the closed state with ATP and maltose-MBP bound or by adding ADP-Mg^{2+} directly to the transporter with maltose-MBP present. Interestingly, our distance measurements (Table 2) agreed reasonably well with the three conformational states seen in crystals of the isolated MalK dimer (Fig. 1*B*). In the absence of nucleotide, the MalK dimer crystallized in both open and semi-open configurations. The semi-open conformation was also obtained in the presence of ADP-Mg^{2+} (21). The ATP-bound dimer was closed (18). Our results are also consistent with two

structures of intact $MalFGK_2$, one closed with ATP-bound (10) and the other open without nucleotide (Khare *et al.*, unpublished data).

Our findings, taken together with recent work (10, 15), further clarify the catalytic cycle of the maltose transporter that appears to occur in two major steps. In studies using EPR to monitor the opening and closing of MBP in the catalytic cycle, we showed that binding of ATP or AMP-PNP-Mg^{2+} triggers high-affinity binding of MBP to the transporter and opening of MBP (15). Knowing that MBP is required to close the nucleotide-binding interface, we can now say that the opening of MBP and the ATP-driven closure of MalK occur in a concerted motion to generate the conformational intermediate captured in the crystal of $MalFGK_2$ (E159Q) with ATP, maltose, and MBP bound (first step). As shown in the structure (10), this concerted motion results in the release of maltose from MBP into a sugar-binding site halfway through the membrane. Furthermore, the work of Austermuhle indicates that ADP-Mg^{2+} (or ATP-Mg^{2+}) fails to trigger the tight-binding and opening of maltose-bound MBP (15), although according to our data, the MalK dimer will progress to a semi-open configuration if MBP is present. Therefore, the opening or closing of MBP must coincide with motions between the semi-open and the closed conformation of the MalK dimer rather than between the open and the semi-open configurations. The importance of the γ-phosphate in stabilizing this conformational transformation is clear because ATP, but not ADP, can stabilize it. After ATP hydrolysis, there must be a large decrease in affinity for this phosphate because the interface opens under these conditions. This decrease in free energy is likely associated with the final translocation of maltose into the cell because the release of P_i will be accompanied by the opening of MalK dimer to the semi-open conformation, the reorientation of TM helices that exposes the sugar-binding site to the cytoplasm, and the closure of MBP (second step). Dissociation of MBP and/or release of ADP-Mg^{2+} may trigger a further opening of the nucleotide-binding interface to prepare for the next cycle of ATP binding and translocation. In summary, we propose that two major steps, closure of the nucleotide-binding interface to hydrolyze ATP and opening to release P_i, coincide with global conformational changes needed to move maltose across the membrane. To the best of our knowledge, the second step has not yet been clearly correlated with substrate transport in the ABC family and is worthy of additional investigation. Interestingly, P_i release has recently been shown to be associated with an important conformational change in the catalytic cycle of another motor protein, the F_1-ATPase. This enzyme rotates in three 120° steps, each associated with one cycle of ATP binding and hydrolysis. ATP binding causes the first 80° of rotation, and the second 40° of rotation is associated with P_i release (28, 29).

Materials and Methods

Construction of a Cysteine-Free Transporter and Introduction of New Cysteines. A cysteine-free version of $MalFGK_2$ has been described (30); however, the level of expression was not suitable for use in EPR experiments. The low yield was traced to the use of pSSB1 encoding cysteine-free MalK (C40G, C252S, C362S). Therefore, another version of cysteine-free MalK was created from the plasmid pKJ, which overexpresses the WT MalK with a C-terminal histidine tag (18). Site-directed mutagenesis was performed by using the GeneTailor Kit (Invitrogen), and primers were designed according to the manufacturer's instructions. MalK containing either C352S or C352A substitutions was well expressed, and a mutagenic primer containing a mixture of bases (AGTC/TC/AG) was used to replace C362 (TGT) with a variety of other amino acids. The combination C352S/C362M was well expressed. Finally, C40 was replaced with Gly, Ser, or Ala, and the Ser substitution was best tolerated. The optimized plasmid, pCO-SSM, containing C40S, C352S, and C362M substitutions, complemented a deletion of the *malK* gene (Δ*malB*214) (31), as judged on maltose MacConkey agar (Difco) (32). The cysteine-free transporter, expressed from the combination of pMR81 (encoding cysteine-free MalF/MalG) (30) and pCO-SSM, can be routinely purified at 2 mg/liter of culture and displays a MBP-stimulated ATPase activity at 80% of the WT. Mutations V16C, R129C, and W13C were individually introduced in pCO-SSM. A plasmid encoding the double mutant V16C/R129C was produced by restriction digestion (HindIII and MluI) of the plasmids carrying the single mutations and religation of the appropriate fragments after gel extraction. *MalK* sequences were verified by DNA sequencing.

Purification and Spin-Labeling of $MalFGK_2$ Mutant Transporters. *E. coli* strain HN741 transformed with pMS421 (spectinomycin) (33), pMR81 (ampicillin), and pCO-SSM containing the desired mutation(s) (chloramphenicol) was grown in TB media at 37°C to OD_{600} ≈0.5. Expression was then induced with 0.01 mM isopropyl-β-D-thiogalactopyranoside, and cells were grown overnight at 23°C. Cells were harvested by centrifugation at 5,000 × *g* for 10 min, washed with TE buffer (50 mM Tris/1 mM EDTA, pH 8) at 4°C, resuspended in TE buffer, and frozen at −80°C (≈35 ml/liter of culture) for at least 1 h. After adding 5 mM $MgCl_2$, 5 μg/ml DNase, and 2 mM DTT, the cells were lysed by two passages through a French press (18,000 psi). After centrifugation (8,000 × *g* for 20 min), the resulting supernatant was centrifuged at 100,000 × *g* for 1 h at 4°C. Pelleted membranes were resuspended in TE, centrifuged again, resuspended in 20 mM Hepes pH 7.5, 20% glycerol, and 5 mM $MgCl_2$, and frozen at −80°C until use. Membranes were diluted to 3–4 mg/ml in 20 mM Hepes pH 7.5, 300 mM NaCl, 10% glycerol, and incubated at 4°C in the presence of 1% of *n*-dodecyl-β-D-maltoside (DDM) for 30 min, with gentle mixing. After a centrifugation at 100,000 × g for 1 h at 4°C, the supernatant was incubated with 100 μM of MTSL (Toronto Research Chemicals) for 1 h at 4°C and then with Talon affinity resin (Clontech), preequilibrated with buffer containing 20 mM Hepes pH 7.5, 300 mM NaCl, 10% glycerol, and 0.01% DDM for 1 h at 4°C, with gentle mixing. The mixture was placed into a column and washed with equilibration buffer containing 5 mM imidazole until OD_{280} of fractions was <0.02. Then the transport complex was eluted in the same buffer containing 100 mM imidazole. Samples were dialyzed overnight at 4°C in 20 mM Tris·HCl pH 8, 150 mM NaCl, 10% glycerol, and 0.01% DDM and then concentrated with centrifugal filter devices (Millipore, cut off 100 kDa), aliquoted, and frozen at −80°C. A gel filtration chromatography step was added (10) to increase the purity of mutants used for spin–spin interaction.

Purification of MBP. MBP was prepared as described in ref. 15.

Assay of ATPase Activity. Proteins were reconstituted into proteoliposomes for activity assays. L-α-phosphatidylcholine (Sigma; P5638), stored under nitrogen at −20°C at 50 mg/ml in 20 mM Tris·HCl pH 8, was thawed and sonicated to clarity in a closed glass tube. Typically, 200 μl of sonicated lipids were preincubated with 20 μl of a 15% stock solution of octyl-β-D-glucopyranoside for 10 min at room temperature, then added to 100 μg of transporter from a 1.3 mg/ml stock solution and incubated for 10 min on ice (lipid to protein weight ratio 100:1). Proteoliposomes were formed after a fast dilution directly into the ATPase mixture (>20-fold dilution). ATPase activities were recorded at 22°C by using an ATP-regenerating system coupled to the disappearance of NADH at 340 nm (34). Typically, 3 μg of transporter were added to the ATPase mixture (50 mM Hepes/KOH pH 8, 10 mM $MgCl_2$, 4 mM phosphoenol pyruvate, 60 μg/ml pyruvate kinase, 32 μg/ml lactate dehydrogenase, 0.3 mM NADH, 1.5 mM ATP, in presence or absence of 150 μM maltose and 2.5 μM MBP), and the rate of ATP hydrolysis was monitored for 10 min. The presence of $MgCl_2$, in excess of ATP, is used to permeabilize the membrane bilayer because ATP and MBP interact on opposite sides of the transporter (35).

EPR Spectroscopy. X-band EPR spectroscopy was carried out on a Bruker EMX-plus with an ER 4119HS cavity. Thirty-microliter samples were contained in a glass capillary inserted in a quartz tube. The spectra were recorded at room temperature at 10 mW microwave power and were normally signal averaged nine times. Distance measurements between the two spin-labeled, side chains were obtained by using simulation software written in LabVIEW by Dr. C. Altenbach (23). Briefly, the broadening function, resulting from spin–spin interactions, was obtained from a Fourier deconvolution procedure. A weighted sum of Pake functions corresponding to the interspin distances is obtained by fitting to the broadening function. A simulated spectrum from this distribution of distances is compared with the experimental spectrum for validation. Technical details and experimental examples are provided in ref. 23. The labeling efficiency was determined by comparison of the amount of spin incorporated into the protein (double integral of the signal) with a standard containing 100 μM free MTSL. The protein concentration was determined by the BioRad Protein Assay.

Sample Conditions for EPR Spectroscopy. Protein samples in detergent were used at a concentration ranging from 75 to 140 μM in dialysis buffer. Samples

were incubated with one or more of the following compounds for 15 min at room temperature before recording spectra: 2.5 mM EDTA, 15 mM ATP, 1 mM maltose, 200 μM MBP, 13 mM AMP-PNP, or 10 mM $MgCl_2$. Protein samples reconstituted into liposomes were prepared by using essentially the same procedure as described for the ATPase assay except at a 50:1 lipid-to-protein weight ratio; 100 μl of sonicated lipids were mixed with 10 μl of octyl-β-D-glucopyranoside, then added to 100 μg of transporter (2.6 mg/ml). Proteoliposomes were formed after a 20-fold dilution into 20 mM Tris·HCl pH 8. The solution was subjected to centrifugation at 100,000 $\times$ g for 3 h at 4°C. Proteoliposomes were resuspended in a small volume of 20 mM Tris·HCl pH 8 and used directly for EPR.

ACKNOWLEDGMENTS. This work is dedicated to the memory of Damien Lehalle. We thank J. Chen for critical reading of the manuscript and F. Alvarez, J. Cui, D. Boudreaux, M. Park, A. Orelle, K. Solka, D. Khare, M. Oldham, O. Dalmas for support and helpful discussions. C.O. thanks S. Qasim for preparation of MBP and M. Oldham for assistance in exclusion chromatography. This work was supported by National Institutes of Health Grant GM-49261, National Biomedical EPR Center Grant EB001980, and the Robert A. Welch Foundation. Sequencing data were acquired in the Purdue Cancer Center sequencing facility supported by National Cancer Institute Cancer Center Support Grant CA23168 to the Purdue Cancer Center. C.O. is a recipient of a postdoctoral fellowship from Fondation pour la Recherche Médicale.

1. Holland IB, Blight MA (1999) ABC-ATPases, adaptable energy generators fuelling transmembrane movement of a variety of molecules in organisms from bacteria to humans. *J Mol Biol* 293:381–399.
2. Gillet JP, Efferth T, Remacle J (2007) Chemotherapy-induced resistance by ATP-binding cassette transporter genes. *Biochim Biophys Acta* 1775:237–262.
3. Lage H (2003) ABC-transporters: Implications on drug resistance from microorganisms to human cancers. *Int J Antimicrob Agents* 22:188–199.
4. Borst P, Elferink RO (2002) Mammalian ABC transporters in health and disease. *Annu Rev Biochem* 71:537–592.
5. Jones PM, George AM (2004) The ABC transporter structure and mechanism: Perspectives on recent research. *Cell Mol Life Sci* 61:682–699.
6. Moody JE, Millen L, Binns D, Hunt JF, Thomas PJ (2002) Cooperative, ATP-dependent association of the nucleotide binding cassettes during the catalytic cycle of ATP-binding cassette transporters. *J Biol Chem* 277:21111–21114.
7. Hopfner KP, *et al.* (2000) Structural biology of Rad50 ATPase: ATP-driven conformational control in DNA double-strand break repair and the ABC-ATPase superfamily. *Cell* 101:789–800.
8. Smith PC, *et al.* (2002) ATP binding to the motor domain from an ABC transporter drives formation of a nucleotide sandwich dimer. *Mol Cell* 10:139–149.
9. Hollenstein K, Dawson RJ, Locher KP (2007) Structure and mechanism of ABC transporter proteins. *Curr Opin Struct Biol* 17:412–418.
10. Oldham ML, Khare D, Quiocho FA, Davidson AL, Chen J (2007) Crystal structure of a catalytic intermediate of the maltose transporter. *Nature* 450:515–521.
11. Fetsch EE, Davidson AL (2002) Vanadate-catalyzed photocleavage of the signature motif of an ATP-binding cassette (ABC) transporter. *Proc Natl Acad Sci USA* 99:9685–9690.
12. Szakacs G, Ozvegy C, Bakos E, Sarkadi B, Varadi A (2001) Role of glycine-534 and glycine-1179 of human multidrug resistance protein (MDR1) in drug-mediated control of ATP hydrolysis. *Biochem J* 356:71–75.
13. Tombline G, Bartholomew L, Gimi K, Tyndall GA, Senior AE (2004) Synergy between conserved ABC signature Ser residues in P-glycoprotein catalysis. *J Biol Chem* 279:5363–5373
14. Verdon G, *et al.* (2003) Formation of the productive ATP-Mg^{2+}-bound dimer of GlcV, an ABC-ATPase from Sulfolobus solfataricus. *J Mol Biol* 334:255–267.
15. Austermuhle MI, Hall JA, Klug CS, Davidson AL (2004) Maltose-binding protein is open in the catalytic transition state for ATP hydrolysis during maltose transport. *J Biol Chem* 279:28243–28250.
16. Davidson AL, Shuman HA, Nikaido H (1992) Mechanism of maltose transport in Escherichia coli: Transmembrane signaling by periplasmic binding proteins. *Proc Natl Acad Sci USA* 89:2360–2364.
17. Chen J, Sharma S, Quiocho FA, Davidson AL (2001) Trapping the transition state of an ATP-binding cassette transporter: Evidence for a concerted mechanism of maltose transport. *Proc Natl Acad Sci USA* 98:1525–1530.
18. Chen J, Lu G, Lin J, Davidson AL, Quiocho FA (2003) A tweezers-like motion of the ATP-binding cassette dimer in an ABC transport cycle. *Mol Cell* 12:651–661.
19. van der Does C, Presenti C, Schulze K, Dinkelaker S, Tampe R (2006) Kinetics of the ATP hydrolysis cycle of the nucleotide-binding domain of Mdl1 studied by a novel site-specific labeling technique. *J Biol Chem* 281:5694–5701.
20. Zaitseva J, *et al.* (2005) Functional characterization and ATP-induced dimerization of the isolated ABC-domain of the haemolysin B transporter. *Biochemistry* 44:9680–9690.
21. Lu G, Westbrooks JM, Davidson AL, Chen J (2005) ATP hydrolysis is required to reset the ATP-binding cassette dimer into the resting-state conformation. *Proc Natl Acad Sci USA* 102:17969–17974.
22. Rabenstein MD, Shin YK (1995) Determination of the distance between two spin labels attached to a macromolecule. *Proc Natl Acad Sci USA* 92:8239–8243.
23. Altenbach C, Oh KJ, Trabanino RJ, Hideg K, Hubbell WL (2001) Estimation of inter-residue distances in spin labeled proteins at physiological temperatures: Experimental strategies and practical limitations. *Biochemistry* 40:15471–15482.
24. Reich-Slotky R, Panagiotidis C, Reyes M, Shuman HA (2000) The detergent-soluble maltose transporter is activated by maltose binding protein and verapamil. *J Bacteriol* 182:993–1000.
25. Geourjon C, *et al.* (2001) A common mechanism for ATP hydrolysis in ABC transporter and helicase superfamilies. *Trends Biochem Sci* 26:539–544.
26. Ivetac A, Campbell JD, Sansom MS (2007) Dynamics and function in a bacterial ABC transporter: Simulation studies of the BtuCDF system and its components. *Biochemistry* 46:2767–2778.
27. Tombline G, Senior AE (2005) The occluded nucleotide conformation of p-glycoprotein. *J Bionenerg Biomembr* 37:497–500.
28. Adachi K, *et al.* (2007) Coupling of rotation and catalysis in F(1)-ATPase revealed by single-molecule imaging and manipulation. *Cell* 130:309–321.
29. Senior AE (2007) ATP synthase: Motoring to the finish line. *Cell* 130:220–221.
30. Samanta S, *et al.* (2003) Disulfide cross-linking reveals a site of stable interaction between C-terminal regulatory domains of the two MalK subunits in the maltose transport complex. *J Biol Chem* 278:35265–35271.
31. Raibaud O, Roa M, Braun-Breton C, Schwartz M (1979) Structure of the malB region in *Escherichia coli* K12. I. Genetic map of the malK-lamB operon. *Mol Gen Genet* 174:241–248.
32. Miller JH (1972) *Experiments in Molecular Genetics* (Cold Spring Harbor Lab Press, Cold Spring Harbor, NY).
33. Davidson AL, Sharma S (1997) Mutation of a single MalK subunit severely impairs maltose transport activity in *Escherichia coli*. *J Bacteriol* 179:5458–5464.
34. Scharschmidt BF, Keeffe EB, Blankenship NM, Ockner RK (1979) Validation of a recording spectrophotometric method for measurement of membrane-associated Mg- and NaK-ATPase activity. *J Lab Clin Med* 93:790–799.
35. Liu CE, Liu PQ, Ames GF (1997) Characterization of the adenosine triphosphatase activity of the periplasmic histidine permease, a traffic ATPase (ABC transporter). *J Biol Chem* 272:21883–21891.